

BIOMECHANICAL AND BIOCHEMICAL CELLULAR RESPONSE DUE TO SHOCK WAVES

James Barthel, Samidha Konkar, Georgy Sankin, Pei Zhong*, and Stefan Zauscher*
Department of Mechanical Engineering and Materials Science, Duke University, Durham, NC 27708

Eric Darling and Farshid Guilak*
Departments of Surgery and Biomedical Engineering, Duke University Medical Center, Durham, NC 27710

Chian-Fong Yen and Bryan Cheeseman
United States Army Research Laboratory – Weapons and Materials Research Directorate, Aberdeen Proving Grounds, MD 21005

Bruce LaMattina*
United States Army Research Laboratory – Army Research Office, Research Triangle Park, NC 27709

ABSTRACT

Our research provides a first step towards a systematic, cell-level study of the effects of shock waves on the mechanical and biochemical properties of cells on solid supports. Motivated to better understand the relationship between shock exposure and heterotopic ossification (HO) a type of soft tissue injury, we designed an experimental setup to expose cell sheets of adipose derived stem cells to shock waves. A key guideline in the experimental design was to suppress cavitation. To this end we built a spark transducer and used a pressurized sample chamber. Cell viability tests and cytoskeletal staining showed little difference between shock-exposed cells and controls. We attribute this to the absence of cavitation. Time-resolved gene expression revealed that a large number of genes were affected by the shock wave exposure. Importantly, the experimental setup and the procedures we developed provide a basis for further studies of shock wave effects on a broad range of other cells. Specifically, they could be adopted to gain further understanding of cellular level causes of traumatic brain injury.

1. Introduction

Improved vehicle and body armor used by our military and rapid medical intervention have increased the survival rates in the field. With casualty rates dropping there is, however, an emergence of new and non-lethal, soft-tissue injuries such as traumatic brain injuries (TBI) and heterotopic ossification (HO), which are associated with exposure to blasts. ([Anon] 2006; Hoge et al. 2008; Lew et al. 2005; Potter et al. 2007). While strides are being made to understand the mechanism of blast injuries with biomechanical approaches, still little is known about cellular level damage, including biochemical effects, and the role of cavitation in causing localized injury.

Motivation Our work is motivated by HO, i.e., the development of bone tissue in a non-osseous or soft tissue after soft tissue trauma. This unnatural development of bone has been previously related to trauma taking place during surgery, especially knee and hip surgeries, but current examples of HO are new and are apparently associated with trauma from blast injuries (Anderson et al. 2007; Lindholm et al. 1986; Rumi et al. 2005). Details of the structural and biochemical changes on the cellular level associated with this trauma are still largely unknown. One current theory suggests that HO originates from osteoprogenitor stem cells lying dormant within affected soft tissues. Here we wish to study the effects of shock loading on the biomechanical and biochemical properties of stem cells. Our choice of human derived adipose stem cells (hASCs) as a reasonable model system is motivated by their availability and ability to differentiate into osteoblast type cells Guilak et al. (Guilak et al. 2006).

Our research presented here, provides a first step towards a systematic, cell-level study of the effects of shock waves on the mechanical and biochemical properties of cells on solid supports. Furthermore, the experimental setup and the procedures we developed provide a basis for further studies of shock wave effects on a broad range of other cells. Specifically, they could be adopted to gain further understanding of cellular level causes of traumatic brain injury.

Blasts and Cavitation Blasts often occur through the detonation of explosive materials at or near the ground surface. The peak blast pressures that result from these typically hemispherical explosions are proportional to the charge weight, and decay exponentially as a function of distance from the origin. At sufficiently large distances, the pressure amplitude becomes negative. Blast pressures can be amplified significantly when the shock wave encounters a solid structure or object in its path. Thus,

Report Documentation Page				Form Approved OMB No. 0704-0188	
Public reporting burden for the collection of information is estimated to average 1 hour per response, including the time for reviewing instructions, searching existing data sources, gathering and maintaining the data needed, and completing and reviewing the collection of information. Send comments regarding this burden estimate or any other aspect of this collection of information, including suggestions for reducing this burden, to Washington Headquarters Services, Directorate for Information Operations and Reports, 1215 Jefferson Davis Highway, Suite 1204, Arlington VA 22202-4302. Respondents should be aware that notwithstanding any other provision of law, no person shall be subject to a penalty for failing to comply with a collection of information if it does not display a currently valid OMB control number.					
1. REPORT DATE DEC 2008		2. REPORT TYPE N/A		3. DATES COVERED -	
4. TITLE AND SUBTITLE Biomechanical And Biochemical Cellular Response Due To Shock Waves				5a. CONTRACT NUMBER	
				5b. GRANT NUMBER	
				5c. PROGRAM ELEMENT NUMBER	
6. AUTHOR(S)				5d. PROJECT NUMBER	
				5e. TASK NUMBER	
				5f. WORK UNIT NUMBER	
7. PERFORMING ORGANIZATION NAME(S) AND ADDRESS(ES) Department of Mechanical Engineering and Materials Science, Duke University, Durham, NC 27708				8. PERFORMING ORGANIZATION REPORT NUMBER	
9. SPONSORING/MONITORING AGENCY NAME(S) AND ADDRESS(ES)				10. SPONSOR/MONITOR'S ACRONYM(S)	
				11. SPONSOR/MONITOR'S REPORT NUMBER(S)	
12. DISTRIBUTION/AVAILABILITY STATEMENT Approved for public release, distribution unlimited					
13. SUPPLEMENTARY NOTES See also ADM002187. Proceedings of the Army Science Conference (26th) Held in Orlando, Florida on 1-4 December 2008, The original document contains color images.					
14. ABSTRACT					
15. SUBJECT TERMS					
16. SECURITY CLASSIFICATION OF:			17. LIMITATION OF ABSTRACT UU	18. NUMBER OF PAGES 7	19a. NAME OF RESPONSIBLE PERSON
a. REPORT unclassified	b. ABSTRACT unclassified	c. THIS PAGE unclassified			

0.000e+00
of 4188875
min
U.S. 27 inches L&P
0.000e+00 0.000e+00

Time = 0.0002702
Contours of Pressure
min=-240596, at elev= 3750
max=209366, at elev= 3771

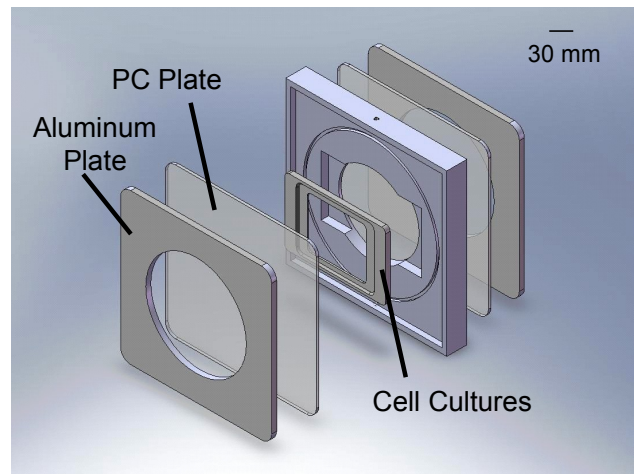
Pressure Levels

- 2.016e+05
- 2.275e+04
- 1.617e+05
- 1.285e+05
- 7.882e+04
- 2.119e+04
- 3.241e+04
- 8.699e+04
- 1.397e+05
- 1.934e+05
- 2.470e+05

Details of these micro- and nanoscale fluid mechanics effects on cells and tissues are only now beginning to be investigated systematically. For example, the cavitation of gas bubbles near rigid surfaces is often asymmetric and can lead to liquid jet formation that can create significant, localized surface damage. Bubble cavitation, and subsequent cell membrane disruption, is a realistic outcome when cells and tissues are exposed to shock waves, for example, cavitation induced damage has been reported for cells when exposed to ultrasonic irradiation (sonoporation) (Ohl et al. 2006; Ohl/Wolfrum 2003) and optically controlled microbubble cavitation (Prentice et al. 2005).

Shock Wave Transducers We constructed and used electromagnetic (Sankin 2003) and spark (Sankin et al.

Cavitation likely occurs when two conditions are met i) a negative pressure must occur and ii) bubble nuclei must be present. Two common methods for suppressing cavitation are thus to eliminate the negative pressure from the shock wave and to eliminate bubble nucleation. We suppressed bubble formation by filtering and degassing the aqueous medium in contact with the adherent cells, and we designed and built a pressure chamber that allowed us to apply a hydrostatic overpressure (0.6 MPa) to the cell-culture (Figure 2).



Tests to assess the ability to suppress cavitation were conducted, under conditions that would later be used in the cell-sheet experiments. The water in the tank and the water used to fill the chamber were degassed to 4 ppm O_2 and heated to 37°C. The cell culture cassette (OptiCell, see below) was filled with culture media and left in the incubator for 24 hrs, prior to experiments. Cavitation events were detected with a Phantom v7.2 high speed camera and a Passive Cavitation Detector (PCD) (Cleveland et al. 2000; Zhong et al. 1997). The high speed camera was configured to have a frame rate of 13,333 frames/s (75 μ s between each frame) and a window size of 45 x 45 mm with a resolution of 180 μ m/pixel. The PCD was positioned such that its focal point was aligned with the center of the OptiCell, but faced the surface at an angle of 45° to reduce low frequency noise from the shock wave. Signal noise was further reduced by filtering

the signal with a band pass filter. Images from the high speed camera taken right before the majority of bubbles collapsed were used to measure the average size of bubbles, the bubble cloud diameter, and the bubble density within that cloud (bubbles/cm²). Each data point was an average of five measurements obtained with the “NIH Image-J” image analysis program. Finally, the PCD data was used to calculate the intensity of the bubble collapse. This intensity was calculated from the area under the bubble collapse peak, using the squared and smoothed data.

Pressure A fiber optic probe hydrophone (FOPH) was used to characterize the pressure wave from the electromagnetic and spark transducers. Detailed information on the operation of the FOPH can be found in Chavko *et al.* (Chavko et al. 2007).

Cell Culture Human, adipose derived stem cells (two million at passage two) were purchased from ZenBio (Super lot #25). These cells were expanded twice to yield 25 million cells at passage four and then were cryogenically frozen in liquid nitrogen. Vials containing approximately two million cells were thawed as needed and expanded one more time to passage five for use in tests. To preserve sterility of the cell culture during shock exposure and to accommodate the requirement of static over pressure, a sealable cell culture device, OptiCell (NUNC Brand, Rochester NY) was employed in all experiments. Cells were added to OptiCells directly after expansion and cultured to confluence over three days. The media used to expand the cells consisted of 89% Dulbecco’s Modified Eagle Media F-12 (DMEM-F12) (Biowhittacker 12-719F), 10% Fetal Bovine Serum (FBS) (ZEN BIO FBS04 2B), 5ng/mL Epidermal Growth Factor (EGF) (Rosche 1376454), 1ng/mL Fibroblast Growth Factor (FGF) (Rosche 1123149), 10µg/mL Transforming Growth Factor β1 (TGF-β1) (R and D Systems), and 1% 100x penicillin-streptomycinfungizone (PSF) (GIBCO 15240-062).

Viability Testing The cytotoxicity kit for Mammalian Cells (Invitrogen, L3224) was used to perform live/dead staining of the cells. Calcein AM permeates cells and is converted enzymatically to green fluorescing Calcein in live cells. Ethidium Homodimer-1 (EthD-1) permeates dead cells and fluoresces orange when it contacts DNA. A fluorescent microscope (Axiovert 200, Zeiss, Thornwood NY), equipped with a mercury lamp for excitation and an Axio Cam for imaging was used to image the cells. Images of the live and dead cells were taken at nine, different, shock-exposed positions on each OptiCell.

Cytoskeletal Staining Control and shocked cells were fixed and co-stained with Alexa fluor 647-phalloidin (actin binding) and Cy-3 labeled mAb for vimentin.

Gene Array Analysis Gene expressions for control and shocked cells were evaluated by the Duke Microarray Facility via a spotted DNA microarray encompassing 36,000 human genes (HO36K). In preparation, mRNA was extracted from the lysate of each sample and subsequently reverse transcribed into cDNA before use in microarray analysis. Sample cDNA and a universal control were labeled with two different fluorescent dyes, mixed, and hybridized to a single microarray. Relative intensities of each fluorophore were used in a ratio-based analysis to identify genes that were up- or down-regulated by a factor of two or more.

3. RESULTS AND DISCUSSION

Experimental Setup Our experimental setup, schematically shown in Figure 3, built heavily on instrumentation developed for shock wave lithotripsy (SWL). shock waves from modified SWL shock sources typically have peak pressures of a few MPa and durations of a few tens of microseconds, and are thus higher and shorter than those typically found in blasts in the field. The effects of lithotripter shock waves on the survival and molecular uptake of cells have been investigated in previous studies by Zhong *et al.* (Zhong et al. 1999), Ohl *et al.* (OhlWolfrum 2003), Junge *et al.* (Junge et al. 2003), Lokhandwalla *et al.* (Lokhandwalla et al. 2001), and Sapozhnikov *et al.* (Sapozhnikov et al. 2002). The principal differences between these studies and our own is that our study focuses on characterizing the effects of plane shock waves on adherent stem cell cultures while controlling cavitation whereas previous lithotripsy studies focused on effects of focused shock waves on cell suspensions of cancer or kidney cells.

Cavitation was quantified by measuring bubble size, cloud size, and bubble density using images from the high speed camera. Only bubble density showed a discernible dependence on applied overpressure; i.e., the bubble density decreased with increasing overpressure (Figure 4A). Furthermore, cavitation collapse intensity was measured with the PCD. Cavitation intensity increased with increasing peak tensile pressure and decreased with increasing overpressure (). Extrapolation reveals that overpressures of 0.76 MPa, 1.41 MPa, and 2.43 MPa at 6 kV, 7 kV, and 8 kV, respectively are required to reduce cavitation to below the noise level.

Biomechanical and Biochemical Effects

We investigated the effect of shock waves on (1) cell viability, (2) cytoskeletal integrity, and (3) changes in

gene expression. Initial shock loading tests were conducted on confluent cells cultured in a standard Petri dish, using an electromagnetic transducer that produced a negative pressure of -4 MPa. This setup and transducer caused significant cavitation were cells at the periphery of the collapse area did not survive (Figure 4). To reduce cavitation, we used a spark transducer with similar shock wave peak pressures and durations as the electromagnetic transducer (16MPa and 1.6 μ s), but without the tensile component in all subsequent experiments. To further reduce cavitation tendency, we used an overpressure of 2.7 atm. Shocked cells were compared to a control group which is subjected to identical conditions excluding the shock waves.

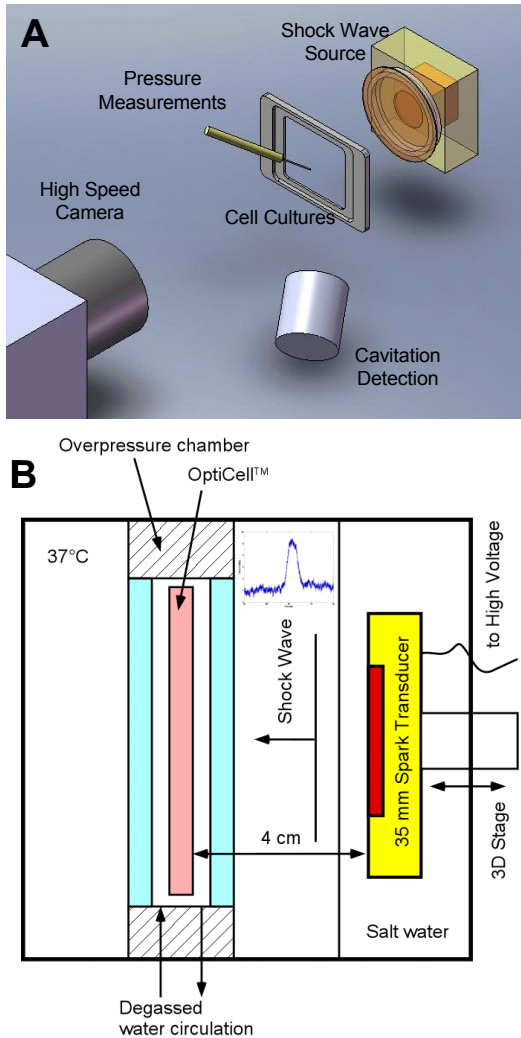


Figure 3: A) Schematic overview of test setup, showing the components. B) Details of the positioning of transducer, overpressure chamber and OptiCell.

(1) Cell Viability Viability tests with suppression of cavitation showed that little to no cell death occurred.

The most dramatic result with respect to cell death is shown in Figure 6. We found that the amount of cell death does not depend on position within the OptiCell for any of the tests performed. The ellipsoidal areas where no cells are present in the live staining (Figure 6) are thought to be places where cell attachment to the substrate was weak. While areas of cell detachment could also be characteristic of cavitation, we do not see any correlation between stain contour and the cells that line the edges of the cavitation area. Furthermore, if cavitation were the cause for these areas they would not be present in the control.

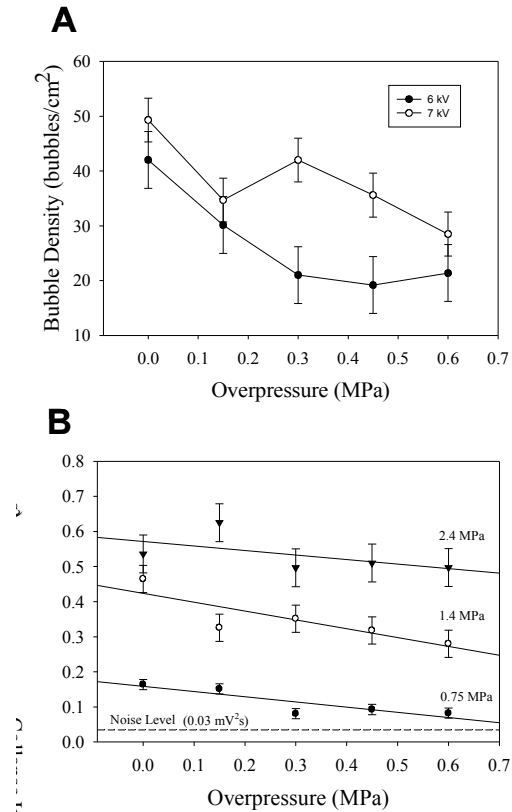


Figure 4: A) bubble density and B) cavitation collapse intensity plotted as a function of overpressure (electromagnetic transducer).

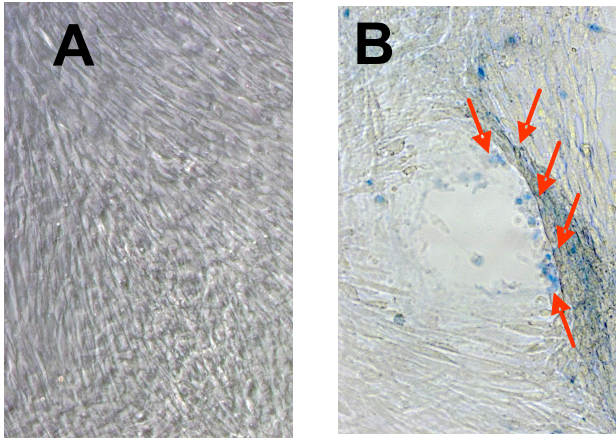


Figure 5: Viability test of adherent hASCs, using the electromagnetic transducer before (A) and after (B) shock exposure. Trypan blue staining shows dead cells in the periphery of area affected by cavitation collapse (red arrows).

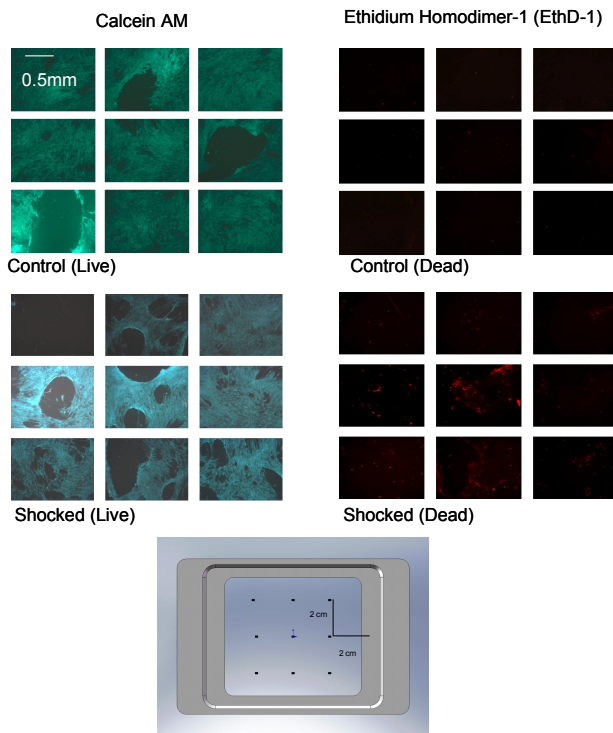


Figure 6: Fluorescence micrographs of control and shocked cells after 10 shocks with the spark transducer at 9kV excitation voltage and 45 degree impingement angle between the transducer and OptiCell faces. The insert below the micrographs schematically shows the locations on the OptiCell where images were acquired.

(2) Cytoskeletal Effects Although cell viability may have not been affected noticeably in our experiments, shock exposure could also affect cytoskeletal structure.

Moosavi-Nejad *et al.* (Moosavi-Nejad et al. 2006) studied the effects of shock wave on the morphology and cytoskeletal deformations in a human renal carcinoma cell line. Their work showed that shock exposure was related to disorganization of the intracellular cytoskeletal filaments; specifically, actin and tubulin showed dramatic rearrangements while vimentin showed no change after shock treatment. We note that these changes in cytoskeletal structure were closely correlated with cell detachment suggesting that cavitation likely played a role, since the local shock intensity is much larger at sites of cavitation than elsewhere. Thus, their experimental conditions were significantly different than ours, where cavitation is suppressed. Our results of microfilament and intermediate filament staining (Figure 7) show no significant difference in the staining pattern between shocked and control cells.

(3) Gene expression Microarray analysis was performed on both the shocked and control samples, and in a survey analysis, over 30,000 genes were initially examined. We analyzed cells harvested 30 minutes and 5 hours after shock exposure at an impingement angle of 0 degree.

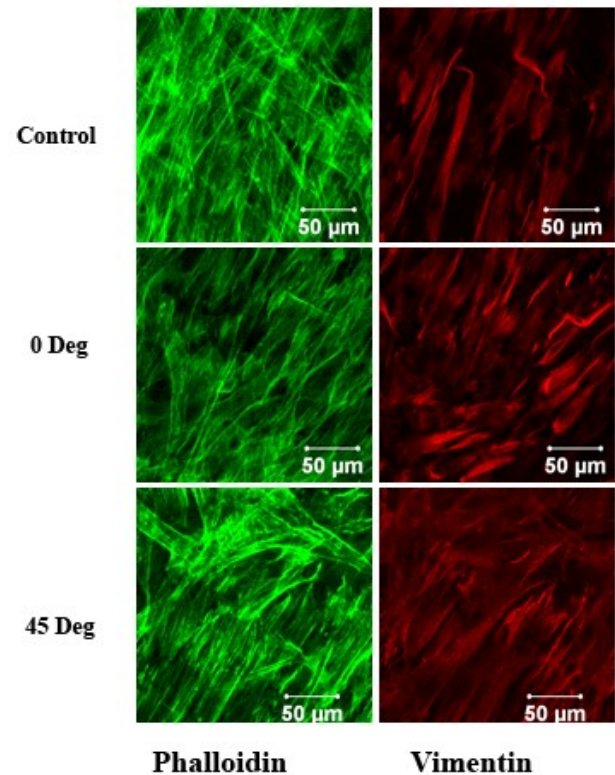


Figure 7: Cells shocked, fixed and labeled with fluorescently labeled phalloidin (actin binding molecule) and anti-vimentin antibody. Control (no shock treatment), and shock impingement at 0 and 45 degrees (10 consecutive shocks with the spark transducer at 9 kV excitation).

We used the computational tool GATHER (Gene Annotation Tool to Help Explain Relationships) to analyze lists of genes identified in our high throughput experiments. We found that in the biological process category, genes controlling phosphorus metabolism, chromatin modification, and integrin-mediated signaling pathway were affected ($p < 0.1$). In the cellular component category, genes associated with the peroxisome, lysosome, microfilaments, nuclear pores, and the plasma membrane were affected ($p < 0.1$). If the expression of the shocked cells was either 2-fold higher or 2-fold lower as compared to control samples, the genes were marked for further analysis. Microarray data showed that a considerable number of genes exceeded this threshold including a few osteogenic related genes (Table 1). In addition to the number of genes that exceeded the selection criteria there were several genes that exhibited a relatively large change in magnitude corresponding to more than 100 times that of the control group. The analysis was performed 30 minutes and 5 hours after the shock exposure to examine the temporal response of the cells. The largest number of cells affected corresponded to the shear wave after 30 minutes. Detailed analysis of the microarray data is continuing.

Table 1: Genes involved in osteogenesis.

Name	Symbol	Exp. Cond. 0 deg. 0.5 h	Exp. Cond. 0 deg. 5 h	Role
Runt-related transcription factor 2	runx2	2.14 ↓	2.86 ↓	Osteoblast-specific transcription Factor
Bone morphogenetic protein 6	VGR1	—	2.95 ↑	Induces the growth of bone and cartilage
Tuftelin 1	TUFT1	—	2.22 ↓	Development and mineralization of enamel
Mitogen activated protein kinase-12	DLK, MULK	2.57 ↓	2.61 ↓	Triggered by external stimuli such as heat shock, osmotic shock

CONCLUSIONS

We designed an experimental setup to expose cell sheets of adipose derived stem cells to shock waves that approximate the intensity of explosions in the field. A key guideline in the experimental design was to suppress cavitation. To this end we built a spark transducer and

used a pressurized sample chamber. Through the use of sealed cell culture cassettes, the sterility of the cells was maintained even in the non-sterile conditions during shock treatment. Cell viability tests and cytoskeletal staining showed little difference between shock-exposed cells and controls. We attribute this to the absence of cavitation (which likely would increase the local shock intensity and strain) and to the limited the amount of strain generated in the 2-dimensional cell sheet configuration. Time-resolved gene expression revealed that a large number of genes were affected by the shock wave and several genes exhibited more than a 100-fold increase or decrease in activity. This initial analysis indicates that there are, as expected, cell/gene level changes that result from exposure shock waves. These cell level changes are a function of time and may contribute to injury conditions that may progress slowly over time. Future work, involving 3-D scaffold cell cultures, will be geared towards uncovering cytoskeletal changes after shock exposure and towards time-resolved gene expression analysis, to probe the expression levels for osteogenic-related genes that could potentially lead to increased concentrations of bone morphogenetic proteins. We anticipate that the general experimental setup and procedures developed here could also serve to study the effect of shock waves on neuronal cells, with importance to traumatic brain injury.

ACKNOWLEDGEMENTS

This work was supported through a grant by the Army Research Office (ARO).

REFERENCES

- [Anon], 2006: Improvised explosive devices and traumatic brain injury among soldiers: The real weapons of mass destruction. *Annals of Neurology*, **60**, 13A-14A.
- Anderson, J. F., T. Boike, J. H. Heinzerling, L. Papiez, and R. Timmerman, 2007: Assessing the feasibility of cone-beam CT simulation for prophylaxis of heterotopic ossification following hip surgery. *International Journal of Radiation Oncology Biology Physics*, **69**, S547-S547.
- Chavko, M., W. A. Koller, W. K. Prusaczyk, and R. M. McCarron, 2007: Measurement of blast wave by a miniature fiber optic pressure transducer in the rat brain. *Journal of Neuroscience Methods*, **159**, 277-281.
- Cleveland, R. O., O. A. Sapozhnikov, M. R. Bailey, and L. A. Crum, 2000: A dual passive cavitation detector for localized detection of lithotripsy-induced cavitation in vitro. *Journal of the Acoustical Society of America*, **107**, 1745-1758.
- Guilak, F., K. E. Lott, H. A. Awad, Q. F. Cao, K. C. Hicok, B. Fermor, and J. M. Gimple, 2006:

- Clonal analysis of the differentiation potential of human adipose-derived adult stem cells. *Journal of Cellular Physiology*, **206**, 229-237.
- Hoge, C. W., D. McGurk, J. L. Thomas, A. L. Cox, C. C. Engel, and C. A. Castro, 2008: Mild traumatic brain injury in US Soldiers returning from Iraq. *New England Journal of Medicine*, **358**, 453-463.
- Junge, L., C. D. Ohl, B. Wolfrum, M. Arora, and R. Ikin, 2003: Cell detachment method using shock-wave-induced cavitation. *Ultrasound in Medicine and Biology*, **29**, 1769-1776.
- Lew, H. L., J. H. Poole, S. Alvarez, and W. Moore, 2005: Soldiers with occult traumatic brain injury. *American Journal of Physical Medicine & Rehabilitation*, **84**, 393-398.
- Lindholm, T. S., T. Viljakka, E. Vankka, L. Popov, and T. C. Lindholm, 1986: Development of Heterotopic Ossification around the Hip - a Long-Term Follow-up of Patients Who Underwent Surgery with 2 Different Types of Endoprostheses. *Archives of Orthopaedic and Trauma Surgery*, **105**, 263-267.
- Lokhandwalla, M., J. A. McAteer, J. C. Williams, and B. Sturtevant, 2001: Mechanical haemolysis in shock wave lithotripsy (SWL): II. In vitro cell lysis due to shear. *Physics in Medicine and Biology*, **46**, 1245-1264.
- Moosavi-Nejad, S. F., S. H. R. Hosseini, M. Satoh, and K. Takayama, 2006: Shock wave induced cytoskeletal and morphological deformations in a human renal carcinoma cell line. *Cancer Science*, **97**, 296-304.
- Ohl, C.-D., M. Arora, R. Ikin, N. De Jong, M. Versluis, M. Delius, and D. Lohse, 2006: Sonoporation from Jetting Cavitation Bubbles. *Biophysical Journal*, **91**, 4285-4295.
- Ohl, C. D., and B. Wolfrum, 2003: Detachment and sonoporation of adherent HeLa-cells by shock wave-induced cavitation. *Biochimica et Biophysica Acta-General Subjects*, **1624**, 131-138.
- Potter, B. K., T. C. Burns, A. P. Lacap, R. R. Granville, and D. A. Gajewski, 2007: Heterotopic ossification following traumatic and combat-related amputations - Prevalence, risk factors, and preliminary results of excision. *Journal of Bone and Joint Surgery-American Volume*, **89A**, 476-486.
- Prentice, P., A. Cuschieri, K. Dholakia, M. Prausnitz, and P. Campbell, 2005: Membrane Disruption by Optically Controlled Microbubble Cavitation. *Nature Physics*, **1**, 107-110.
- Rumi, M. N., G. S. Deol, K. P. Singapuri, and V. D. Pellegrini, 2005: The origin of osteoprogenitor cells responsible for heterotopic ossification following hip surgery: an animal model in the rabbit. *Journal of Orthopaedic Research*, **23**, 34-40.
- Sankin, G. N., 2003: A shock-wave generator of a single cavitation bubble. *Instruments and Experimental Techniques*, **46**, 419-423.
- Sankin, G. N., A. P. Drozhzhin, K. A. Lomanovich, and V. S. Teslenko, 2004: A multisite electric-discharge diaphragm generator of shock waves in a liquid. *Instruments and Experimental Techniques*, **47**, 525-528.
- Sapozhnikov, O. A., V. A. Khokhlova, M. R. Bailey, J. C. Williams, J. A. McAteer, R. O. Cleveland, and C. A. Crum, 2002: Effect of overpressure and pulse repetition frequency on cavitation in shock wave lithotripsy. *Journal of the Acoustical Society of America*, **112**, 1183-1195.
- Yen, C.-F., 2008, US Army Reserach Laboratory.
- Zhong, P., I. Cioanta, F. H. Cocks, and G. M. Preminger, 1997: Inertial cavitation and associated acoustic emission produced during electrohydraulic shock wave lithotripsy. *Journal of the Acoustical Society of America*, **101**, 2940-2950.
- Zhong, P., H. F. Lin, X. F. Xi, S. L. Zhu, and E. S. Bhogte, 1999: Shock wave-inertial microbubble interaction: Methodology, physical characterization, and bioeffect study. *Journal of the Acoustical Society of America*, **105**, 1997-2009.